Separation Science and Technology
Publication details, including instructions for authors and subscription information:
http://www.informaworld.com/smpp/title~content=t713708471

Sans Study Of Third Phase Formation In The U(vi)-hno$_3$/tbp-*n*-dodecane System

R. Chiarizia[a]; M. P. Jensen[a]; M. Borkowski[a]; J. R. Ferraro[a]; P. Thiyagarajan[b]; K. C. Littrell[b]
[a] Chemistry Division, Argonne National Laboratory, Argonne, Illinois, USA [b] IPNS Division, Argonne National Laboratory, Argonne, Illinois, USA

To cite this Article Chiarizia, R. , Jensen, M. P. , Borkowski, M. , Ferraro, J. R. , Thiyagarajan, P. and Littrell, K. C.(2003) 'Sans Study Of Third Phase Formation In The U(vi)-hno$_3$/tbp-*n*-dodecane System', Separation Science and Technology, 38: 12, 3313 — 3331

To link to this Article: DOI: 10.1081/SS-120022601

URL: http://dx.doi.org/10.1081/SS-120022601

MARCEL DEKKER, INC. • 270 MADISON AVENUE • NEW YORK, NY 10016

SEPARATION SCIENCE AND TECHNOLOGY
Vol. 38, Nos. 12 & 13, pp. 3313–3331, 2003

SANS Study of Third Phase Formation in the U(VI)-HNO_3/TBP-*n*-Dodecane System[#]

**R. Chiarizia,[1,*] M. P. Jensen,[1] M. Borkowski,[1]
J. R. Ferraro,[1] P. Thiyagarajan,[2]
and K. C. Littrell[2]**

[1]Chemistry Division and [2]IPNS Division, Argonne National Laboratory,
Argonne, Illinois, USA

ABSTRACT

In spite of its technological importance, third phase formation in the extraction of hexavalent actinides from nitric acid solutions into alkane solutions of tri-*n*-butylphosphate (TBP) has received only limited attention. The focus of the few available literature works has been primarily centered on the composition of the third phase and on the stoichiometry of the metal complexes. Very little is known, on the other

---

[#] Work performed under the auspices of the U. S. Department of Energy, Office of Basic Energy Science, Division of Chemical Science (for the part performed at the Chemistry Division of ANL) and Division of Material Science (for the part performed at INPS), under contract No. W-31-109-ENG-38. Accordingly, the U.S. Government retains a non-exclusive, royalty-free license to publish or reproduce the published form of this contribution, or allow others to do so, for U.S. Government purposes.

[*] Correspondence: R. Chiarizia, Chemistry Division, Argonne National Laboratory, Argonne, IL 60439, USA; E-mail: chiarizia@anl.gov.

DOI: 10.1081/SS-120022601 0149-6395 (Print); 1520-5754 (Online)
Published by Marcel Dekker, Inc. www.dekker.com

hand, about the structure and morphology of the third phase species of hexavalent actinides. In the present investigation, the formation of a third phase upon extraction of U(VI) by 20% TBP in deuterated *n*-dodecane from nitric acid solutions was studied. Chemical analyses have shown that U(VI) exists in the third phase as a species having the composition $UO_2(NO_3)_2{\cdot}(TBP)_2{\cdot}HNO_3$. Small-angle neutron scattering measurements on TBP solutions loaded with only HNO_3 or with increasing amounts of U(VI) have revealed the presence, both before and after phase splitting, of relatively large ellipsoidal aggregates with the parallel and perpendicular axes having lengths up to about 64 and 15 Å, respectively. The formation of these aggregates is observed in all cases, that is, when only HNO_3, only $UO_2(NO_3)_2$, or both HNO_3 and $UO_2(NO_3)_2$ are extracted by the TBP solution. Upon third phase formation, the SANS data reveal the presence of smaller aggregates in both the heavy and light organic phase.

Key Words: Third phase; U(VI); TBP.

INTRODUCTION

Third phase formation in solvent extraction is observed when, at high metal and/or mineral acid loading of the organic phase under suitable experimental conditions, the organic phase splits into two layers, the light layer containing most of the diluent and little extractant and metal, and the heavy or "third" phase containing a high concentration of extractant and metal and little diluent. This phenomenon is well known, has been observed in many systems of technological importance, and has been investigated in a number of studies. Third phase formation depends strongly on the type and concentration of the extractant in the organic phase and of the metal and inorganic acid in the aqueous phase, but also on other factors such as type of diluent and temperature. It has traditionally been attributed to lack of sufficient solubility of the metal–ligand complex in the nonpolar organic phase,[1] and to microemulsion behavior.[2] In a recent work, third phase formation has been interpreted and theoretically predicted, at least at an approximate level, using the Flory–Huggins theory of polymer solutions and the theory of regular solutions.[3]

Excellent reviews, one of which is quite recent, have summarized the most important aspects of this phenomenon.[4,5] The main focus in many of the previous works has been on the conditions under which third phase formation is observed and avoided. Preventing third phase formation is of paramount importance in systems of nuclear interest to avoid the potentially catastrophic consequences of accidentally assembling a critical mass of fissionable materials in third phases. Another common objective of works on third phase formation has been to determine the composition of the species present in the heavy organic phase. Very little information, however, is available on structural aspects of third phase formation.

In small-angle neutron scattering studies (SANS) of metal extraction by dialkyl-substituted alkylenediphosphonic acids in toluene, some of the present authors observed the formation of large cylindrical aggregates upon loading the organic phase with progressively higher concentrations of certain metal ions, such as Fe(III) and Th(IV).[6–8] Attempts to further increase the metal concentration in the organic phase eventually led to the separation of a gelatinous material that can be considered as a particular case of third phase. The appearance of this new phase might be interpreted as the final step of an aggregation process involving the organic phase species. Formation of large and elongated aggregates was also observed in the extraction of praseodymium(III) nitrate by octyl(phenyl)-N,N-diisobutylcarbamoylmethylphosphine oxide (CMPO) in various diluents.[9,10] The investigators hypothesized that the aggregation of the metal-extractant complexes may be an intermediate stage between a homogeneous solution of monomers or very small particles, and the separation of a second organic phase. Similar observations have been reported in a recent work on HNO_3 extraction by an alkyl-substituted malonamide extractant in *n*-dodecane.[11] Also in this case, small-angle x-ray scattering measurements revealed the onset of extensive aggregation of the organic phase species when phase splitting was approached.

In an attempt to verify that the formation of large aggregates in the organic phase before phase splitting is a general feature shared by most, if not all, solvent extraction systems, we have started a series of investigations with a main emphasis on structural aspects of third phase formation. In our first study we revisited the U(VI)-HNO_3/tri-*n*-butylphosphate (TBP)-*n*-dodecane system from the standpoint of third phase formation. We chose this system because, in spite of its technological importance, very few detailed studies are available on third phase formation when U(VI) is extracted by alkane solutions of TBP.[12–14] The objective of this work was to obtain information on the morphology of the species present in the organic phase before and after third phase formation.

EXPERIMENTAL

Materials

TBP (Aldrich Chem. Co., Milwaukee, WI, USA) was distilled from CaH_2. Before use, its solutions were contacted with 0.25-M Na_2CO_3 to remove small amounts of mono- and di-butylphosphoric acids possibly present as degradation products. *n*-Dodecane and deuterated dodecane (d_{26}, 98 atom % D, in the following indicated as D-dodecane) were obtained from Aldrich Chem. Co. (Milwaukee, WI, USA). The $UO_2(NO_3)_2 \cdot 6H_2O$ was obtained from Fisher Scientific Co. (Pittsburgh, PA, USA) and used as such. Aqueous solutions were prepared using water from a Mill-Q2 purification system and Ultrex Reagent nitric acid (J. T. Baker Chemical Co., Sanford, ME, USA). All other reagents were of analytical grade and used without further purifications.

Sample Preparation and Characterization

Four series of samples were prepared for the SANS measurements. A 20% (v/v) TBP (0.73 M) in D-dodecane, not contacted with any aqueous phase, was the only sample of series 1. The samples of series 2 (a through c) were prepared by dissolving increasing amounts of solid $UO_2(NO_3)_2 \cdot 6H_2O$ in the 20% TBP solution, to have about 9%, 47%, and 93%, respectively, of TBP bound to U(VI) [assuming a TBP to U(VI) ratio of 2 in the organic phase complex]. These samples did not contain HNO_3. Sample 2c, with an amount of U(VI) approaching TBP saturation, did not split into a heavy and a light organic phase.

Samples 3 (a through e) were prepared by equilibrating, at 23 ± 1°C and at a phase ratio of one, the 20% TBP solution with aqueous phases having progressively higher HNO_3 concentrations (0.5, 2.5, 5.0, 7.5, and 9.7 M, respectively). For sample 3e, after the first equilibration and phase separation, the resulting organic phase was equilibrated with a fresh aliquot of the same aqueous phase. This was done to maximize the HNO_3 concentration in the organic phase. No third phase formation was observed in the preparation of the series 3 samples, as expected from previous works reporting that in the extraction of HNO_3 (no metal cations present) by 20% TBP in kerosene at room temperature, phase splitting is observed only when the aqueous HNO_3 concentration reaches about 14 M.[1]

The samples of the 4 (a through e) series contained varying concentrations of both HNO_3 and U(VI). They were prepared by contacting a small volume of the TBP solution, preequilibrated twice with 10 M HNO_3 (phase ratio = 1), with an equal volume of 10 M HNO_3 solutions containing progressively increasing concentrations of $UO_2(NO_3)_2$ (from 0.040 to 0.66 M). When contacting the 20% TBP organic phase with an aqueous solution that was 0.66 M in $UO_2(NO_3)_2$ and 10.5 M in HNO_3, a third phase was obtained having a volume of about 16% of the original organic phase volume, and a density of

1.21 g/mL (sample 4d). Sample 4e is the light organic phase in equilibrium with the third phase. Sample 4c has the U(VI) limiting organic concentration (LOC), that is, the highest metal concentration in the organic phase that could be achieved under the selected experimental conditions without phase splitting. This sample was obtained by first causing formation of the third phase and then adding very small amounts of lean organic phase and/or water until the third phase disappeared, as indicated by the absence of turbidity in the organic phase.

After centrifugation and phase separation, aliquots of the various phases were analyzed. The HNO$_3$ concentration in the aqueous phases was determined by potentiometric titration to pH $\backsim 6$ with standard base after appropriate dilution and after making the solution 0.2 M in $(NH_4)_2C_2O_4$ to mask the metal. The aqueous U(VI) concentration was determined by ICP-AES. The organic HNO$_3$ and U(VI) were first stripped by contacting an aliquot of the organic phases diluted tenfold with dodecane, with a larger and known volume of 0.1 M $(NH_4)_2C_2O_4$. HNO$_3$, and U(VI) in the stripping solution were then determined as above. The concentration of water in selected samples was determined by Karl Fisher titrations.

In all the samples where no third phase was generated, the equilibrium TBP concentration was assumed to be equal to the initial one, that is, 0.73 M, neglecting small changes of the organic phase volume upon dissolution or extraction of $UO_2(NO_3)_2$ and/or HNO$_3$. The TBP concentration in the heavy and light organic phases resulting from phase splitting were determined, after appropriate sample dilution with regular dodecane and HNO$_3$ and U(VI) stripping, from the distribution ratio (D) of freshly purified ^{233}U (from ANL stocks) between the organic phase samples and 3 M HNO$_3$, by using an ad hoc calibration curve of D_U vs TBP concentration.

SANS Measurements

The SANS measurements were performed at the time-of-flight, small-angle neutron diffractometer (SAND) at the Intense Pulsed Neutron Source of Argonne National Laboratory.[15,16] SAND uses pulsed neutrons with wavelengths in the range 0.5 to 14 Å and a fixed sample-to-detector distance of 2 m. The scattered neutrons are measured by using a 128 × 128 array of position sensitive gas filled $40 \times 40\,\mathrm{cm}^2$ proportional counters, while the wavelengths are measured from the time-of-flight by binning the pulse to 68 constant $\Delta t/t = 0.05$ time channels. The instrument thus provides a useful range of momentum transfer $[Q = (4\pi/\lambda)\sin(\theta)\,(\text{Å}^{-1})$, where θ is half the scattering angle and λ is the wavelength of the probing neutrons] of 0.003 to 0.7 Å^{-1}.

The samples were measured in Suprasil cells (Quaracell Products) with a diameter of 22 mm and a pathlength of 2 mm. The sample container was thermostated at 23 ± 1°C. The reduced data for each sample were corrected for the background from the instrument and the Suprasil cell. The reduced data were placed on an absolute scale using a polymer melt sample containing an equal-volume mixture of deuterated and hydrogenous high molecular weight polystyrenes of known absolute cross-section.[15]

The SANS signals were interpreted using Guinier analysis (ln[I(Q)] vs Q^2).[17] According to this analysis, the slope of the data in a Q range such that $QR_g \leq 1$ provides the radius of gyration, $R_g (R_g = (-3 \ \text{slope})^{1/2})$. R_g is a measure of the spatial extension of the particle and is given by the root-mean-squared distances of all the atoms from the centroid of the scattering particle. For a polydisperse ample, the radius of gyration is a *z*-average of all the scattering species in the sample.

The SANS data were also analyzed using nonlinear least-squares fits to the following form factor for an ellipsoid of rotation[18]:

$$P(Q,a,b) = \int_0^{\pi/2} \frac{3\left[\sin\left(Qr(a,b,\alpha)\right) - Qr(a,b,\alpha)\cos\left(Qr(a,b,\alpha)\right)\right]}{\left(Qr(a,b,\alpha)\right)^3} \sin\alpha \, d\alpha \tag{1}$$

including a multiplicative scale factor for the intensity at Q = 0 and a constant background term to account for incoherent scattering from hydrogen. Here, α is an orientation angle used to integrate overall possible orientations of the particles relative to the incident beam, *a* is the length of the semiaxes pendicular to the axis of rotation, *b* is the length of the semiaxis parallel to the axis of rotation, and

$$r(a,b,\alpha) = a\left(\sin^2\alpha + \frac{b}{a}\cos^2\alpha\right) \tag{2}$$

From the values of *a* and *b*, the radius of gyration, R_g, of the particles was calculated through the relation $R_g = \sqrt{((2a^2 + b^2)/5)}$.

RESULTS AND DISCUSSION

Table 1 summarizes the composition of the organic phases investigated in this work. The table also reports the concentration of TBP that should be

Table 1. Composition of samples for SANS measurements.

Sample	[TBP][a] M	[U][b] M	[HNO$_3$][c] M	[H$_2$O][d] M	[TBP] bound to U M	[TBP] excess M	[HNO$_3$]/[TBP]$_{excess}$
1	0.73	0	0	0.096	0	0.73	0
2a	0.73	0.032	0	ND[e]	0.064	0.67	0
2b	0.73	0.16	0	ND	0.32	0.39	0
2c	0.73	0.34	0	ND	0.68	0.05	0
3a	0.73	0	0.027	ND	0	0.73	0.037
3b	0.73	0	0.30	ND	0	0.73	0.41
3c	0.73	0	0.48	ND	0	0.73	0.66
3d	0.73	0	0.69	ND	0	0.73	0.95
3e	0.73	0	0.74	0.091	0	0.73	1.0
4a	0.73	0.032	0.72	0.081	0.064	0.67	1.1
4b	0.73	0.22	0.28	0.086	0.45	0.28	1.0
4c (LOC)	0.73	0.23	0.27	0.12	0.45	0.28	0.96
4d (third ph.)	1.9	0.93	0.94	0.35	1.9	∽0	—
4e (light ph.)	0.51	0.17	0.21	0.14	0.34	0.17	1.2

[a] Estimated accuracy ± 5%, except for samples 4d and 4e (±10%).
[b] Estimated accuracy ± 5%.
[c] Estimated accuracy ± 10%.
[d] Estimated accuracy ± 20%.
[e] Not determined.

bound to U(VI), based on the assumption that in the organic phase, the metal exists as the $UO_2(NO_3)_2{\cdot}(TBP)_2$ complex, as reported in previous studies,[19] the concentration of the excess TBP [i.e., the TBP not bound to U(VI)], and the ratio of the HNO_3 concentration to that of the excess TBP.

TBP is known to extract HNO_3 from aqueous solutions forming species having the composition $TBP{\cdot}(HNO_3)_i$, with i equal to 1 through 4.[20] Under the experimental conditions of this work (equilibrium aqueous phase $\leq$ 10 M in HNO_3), and within the accuracy level of our analytical determinations, the data in Table 1 indicate that HNO_3 exists in the organic phase predominantly as the 1:1 complex. In fact, in sample 3e, which contains the highest organic HNO_3 concentration achievable extracting the acid from about 10 M aqueous HNO_3, the ratio of organic HNO_3 to TBP concentrations is about 1.

When U(VI) is transferred from aqueous 10 M HNO_3 into TBP solutions where the extractant exists as $TBP{\cdot}HNO_3$ (as in the case of sample 3e), the metal displaces the acid from the phosphoryl group of TBP, and the equilibrium concentration of organic phase HNO_3 decreases accordingly. Within experimental uncertainty, the data in Table 1 show that for each mole of $UO_2(NO_3)_2$ entering the organic phase, two moles of HNO_3 are displaced from it. This is consistent with the hypothesis that the uranium salt forms with TBP the well-known $UO_2(NO_3)_2{\cdot}(TBP)_2$ adduct,[19] while the excess TBP remains in the form of $TBP{\cdot}HNO_3$. In sample 4c, representing the U(VI) LOC condition, about 62% of the TBP is involved in uranium complexation, leaving 38% as the $TBP{\cdot}HNO_3$ species. Attempts to introduce more acid or metal into the organic phase bring about third phase formation.

The important role played by HNO_3 in causing phase splitting is evident when one compares sample 2c with sample 4c. In the former sample, with no HNO_3 present, almost all TBP in solution can be engaged in binding U(VI) without phase problems; in the latter, the presence of HNO_3 in the organic phase allows significantly less U(VI) extraction, and the organic phase splits in two when the LOC is exceeded.

Finally, the data in Table 1 indicate that the third phase (sample 4d) is highly concentrated in TBP, U(VI), and HNO_3, and also has a higher water content than the other samples. The U(VI):TBP:HNO_3 concentration ratios are about 1:2:1, leading to the conclusion that, under the experimental conditions of this work, the composition of the third phase species can be expressed as $UO_2(NO_3)_2{\cdot}(TBP)_2{\cdot}HNO_3$ (neglecting water), in agreement with previous results obtained under similar conditions.[13]

In representing the stoichiometry of the third phase species as $UO_2(NO_3)_2{\cdot}(TBP)_2{\cdot}HNO_3$, we imply that the HNO_3 molecule is not in the primary coordination sphere of the uranyl ion. This is in agreement with previous studies,[12] but in contrast with other studies where it was assumed that the trinitrato complex $HUO_2(NO_3)_3 \cdot (TBP)_2$ exists in the third phase.[13,14] Our conclusion that $UO_2(NO_3)_2 \cdot (TBP)_2 \cdot HNO_3$ is a more appropriate description of the third phase species is based on infrared and visible spectroscopy measurements and on EXAFS studies on samples similar to those of Table 1.[21,22]

As an example of SANS data, Fig. 1 shows the results of the measurements for samples 1 and 2(a, b, c). Similar sets of results have been obtained for all the samples of Table 1. The increasing scattering intensity, I(Q), at the lowest Q values in the data sets of Fig. 1 is the qualitative indication that the size of the solute particles increases progressively as more and more $UO_2(NO_3)_2$ is dissolved in 20% TBP in D-dodecane, up to almost complete saturation of the extractant.

Guinier analysis was used to extract R_g values and the extrapolated scattering intensities at $Q = 0$, I(0), from the SANS data. Since the SANS data

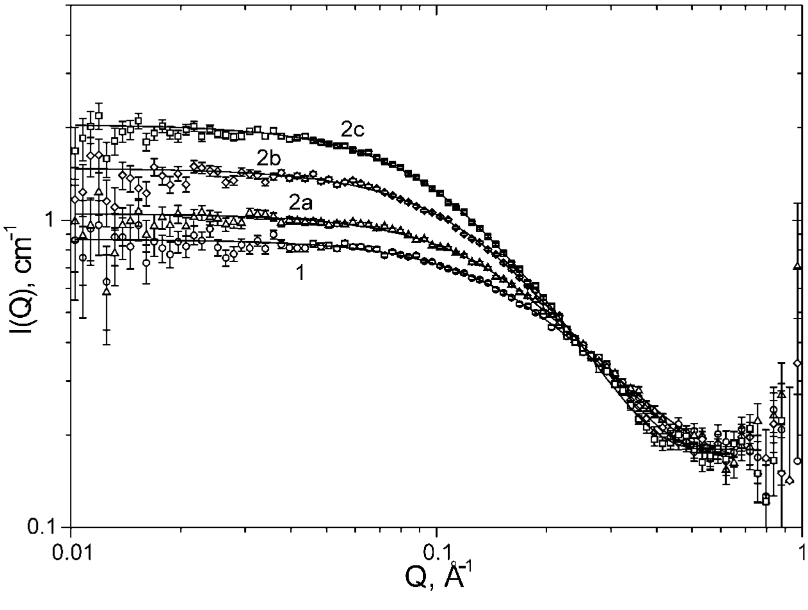

Figure 1. SANS data for samples 1, 2a, 2b, and 2c. For the composition of the samples, see Table 1. The continuous lines represent the ellipsoid of rotation fit of the data.

are available on an absolute scale, the Guinier fit can be used to determine the molecular weight of the extractant aggregates and, hence, the aggregation number of TBP in the aggregates. When the concentration of scattering particles is low and interparticle interactions are negligible, the scattering intensity can be expressed as:

$$I(Q) = N_p(\rho_p - \rho_s)^2 V_p{}^2 P(Q) \tag{3}$$

where P(Q) is the single particle form factor, which describes the angular scattering distribution as a function of particle size and shape,[23] N_p is the number of scattering particles per volume, V_p is the particle volume, and ρ_p and ρ_s are the scattering length densities of the extractant and solvent, respectively. At $Q = 0$, $P(Q) = 1$ and eq. 1 becomes:

$$I(0) = N_p(\rho_p - \rho_s)^2 V_p{}^2 \tag{4}$$

After rearranging and introducing molar quantities in eq. 4, one obtains eq. 5, from which, the weight average aggregation number of TBP, n_w, can be calculated for each sample:

$$n_w = \frac{M_w}{MW_{TBP}} = \frac{6.022 \times 10^{26} d_{TBP}^2 I(0)}{[TBP]_{total}(\rho_p - \rho_s)^2 MW_{TBP}^2} \tag{5}$$

In eq. 5, M_w is the weight average molecular weight of the extractant aggregates, MW_{TBP} and d_{TBP} are the molecular weight (266.32) and the density (0.973 g/mL) of the extractant, and $[TBP]_{total}$ is the total extractant concentration in the organic phase. The scattering length densities of TBP ($\rho_p = 1.566 \times 10^9\,cm^2$) and of D-dodecane ($\rho_s = 6.753 \times 10^{10}\,cm^2$) were calculated from the sum of the scattering length densities of the individual atoms.[6] As the scattering contrast between solute and solvent is essentially determined by the different neutron scattering properties of the H and D atoms, only the highly hydrogenous molecule of TBP was considered in the calculation of ρ_p.

Figure 2 shows, as an example, the Guinier plots for the same samples of Fig. 1. Table 2 reports the values of the gyration radius and TBP aggregation number for all samples. Uncertainties in the n_w values were derived from the uncertainty in I(0) and the assumption of 2% uncertainty in d_{TBP} and 5% uncertainty in $[TBP]_{total}$ (for samples 4d and 4e, the uncertainty in $[TBP]_{total}$ was about 10%).

For a more quantitative interpretation of the SANS data and to obtain information on the shape of the aggregates present in the various samples, the SANS data were fit to an ellipsoid of rotation form factor. Figure 1 shows

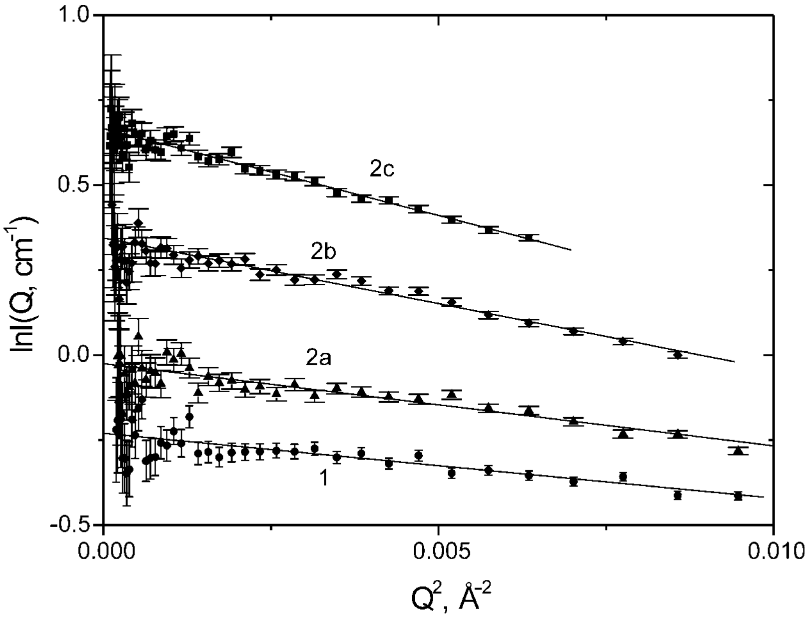

Figure 2. Guinier plots for samples 1, 2a, 2b, and 2c. For the composition of the samples, see Table 1.

Table 2. Gyration radius of solute particles and TBP weight average aggregation number from Guinier analysis.

Sample	R_gÅ	I(0) cm^{-1}	n_w
1	7.6 ± 0.3	0.793 ± 0.004	2.0 ± 0.2
2a	8.5 ± 0.4	0.974 ± 0.006	2.5 ± 0.2
2b	10.8 ± 0.6	1.412 ± 0.008	3.6 ± 0.2
2c	12.4 ± 0.8	1.95 ± 0.01	4.9 ± 0.3
3a	7.9 ± 0.3	0.854 ± 0.004	2.2 ± 0.1
3b	11.7 ± 0.7	1.63 ± 0.01	4.1 ± 0.2
3c	11.6 ± 0.8	1.55 ± 0.01	3.9 ± 0.2
3d	12.4 ± 0.8	1.62 ± 0.01	4.1 ± 0.2
3e	12.3 ± 0.9	2.16 ± 0.02	5.5 ± 0.3
4a	13.0 ± 1.4	2.34 ± 0.02	5.9 ± 0.4
4b	13.6 ± 1.4	1.97 ± 0.02	5.0 ± 0.3
4c (LOC)	15.2 ± 1.4	2.38 ± 0.02	6.0 ± 0.4
4d (third ph.)	9.6 ± 1.0	1.18 ± 0.01	1.1 ± 0.1
4e (light ph.)	12.1 ± 1.3	1.32 ± 0.01	4.5 ± 0.5

Table 3. Ellipsoid of rotation fit of SANS data.

Sample	*a*, perpendicular semiaxis, Å	*b*, parallel semiaxis, Å	R_gÅ	I(0) cm^{-1}	$n_{w,exp}$	$n_{w,calc}$
1	5.1 ± 0.4	17.6 ± 0.3	8.5 ± 0.3	0.70 ± 0.01	1.8 ± 0.2	1.6
2a	5.6 ± 0.2	19.4 ± 0.3	9.4 ± 0.3	0.89 ± 0.01	2.2 ± 0.2	2.2
2b	6.8 ± 0.1	23.5 ± 0.2	11.4 ± 0.2	1.31 ± 0.01	3.3 ± 0.2	3.8
2c	7.8 ± 0.1	28.6 ± 0.2	13.7 ± 0.2	1.87 ± 0.01	4.7 ± 0.3	4.9
3a	5.6 ± 0.3	18.3 ± 0.3	8.9 ± 0.3	0.75 ± 0.01	1.9 ± 0.2	1.9
3b	6.8 ± 0.1	25.8 ± 0.2	12.3 ± 0.2	1.51 ± 0.01	3.8 ± 0.2	3.4
3c	6.6 ± 0.1	27.2 ± 0.3	12.9 ± 0.3	1.44 ± 0.01	3.7 ± 0.2	3.7
3d	7.0 ± 0.1	28.1 ± 0.3	13.3 ± 0.3	1.50 ± 0.01	3.8 ± 0.2	4.0
3e	6.7 ± 0.1	25.9 ± 0.3	12.3 ± 0.3	1.99 ± 0.01	5.0 ± 0.3	5.0
4a	6.7 ± 0.1	27.1 ± 0.2	12.8 ± 0.2	2.14 ± 0.01	5.4 ± 0.4	5.0
4b	7.4 ± 0.1	28.8 ± 0.3	13.7 ± 0.3	1.92 ± 0.01	4.9 ± 0.3	5.0
4c (LOC)	7.5 ± 0.1	32.1 ± 0.3	15.1 ± 0.3	2.30 ± 0.02	5.8 ± 0.4	5.0
4d (third ph.)	6.5 ± 0.3	21.4 ± 0.4	10.4 ± 0.4	0.97 ± 0.01	0.9 ± 0.1	2.0
4e (light ph.)	7.1 ± 0.2	25.2 ± 0.4	12.1 ± 0.3	1.29 ± 0.01	4.7 ± 0.5	5.0

the ellipsoidal fit of the same SANS data shown in Figs. 1 and 2. The fit of the other data sets is not shown here for brevity. For each data set, Table 3 reports the perpendicular (*a*) and parallel (*b*) semiaxes, the gyration radius calculated from the values of the semiaxes, the I(0) value, and the experimental weight average aggregation number of TBP obtained using the I(0) value and eq. 5. Overall, the R_g and I(0) values in Table 3 are very close to those listed in Table 2. This lends support to the validity of the Guinier analysis of the SANS data.

Several results in Table 3 deserve comment. First of all, the R_g values of the solute particles increase steadily as more U(VI) or HNO_3 is introduced in solution, up to a maximum value of 13.7 Å (sample 2c) and 12.3 Å (sample 3e). It seems, therefore, that the extraction of either $UO_2(NO_3)_2$ or HNO_3 has the same effect on particle growth. When $UO_2(NO_3)_2$ is added to a solution that already contains HNO_3, only a modest further growth of the particles is observed, as indicated by the R_g values obtained for samples 4a and 4b. As expected, the largest particles are observed in sample 4c, representing the LOC condition.

Somewhat surprisingly, however, after phase spitting, the R_g value of the third phase sample (4d) reveals that the size of the aggregates has become significantly smaller than in the LOC sample. Actually, the aggregates in the heavy phase seem to be even smaller than those in the light phase (4e).

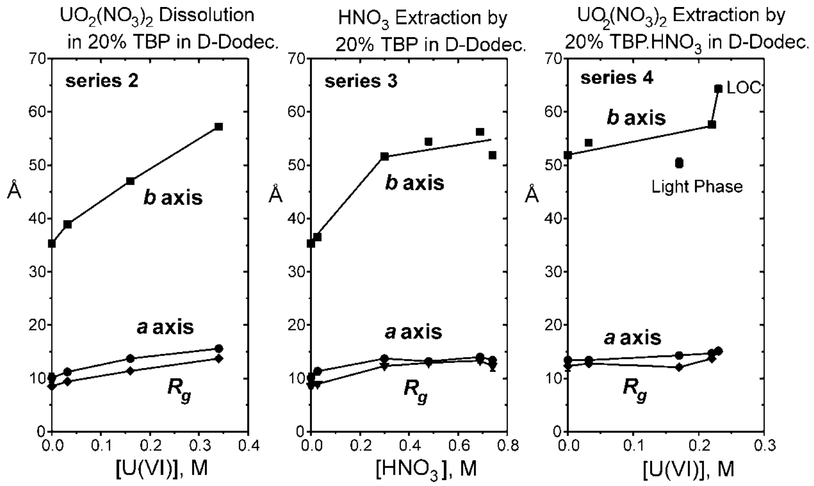

Figure 3. Gyration radius and axes of the ellipsoidal aggregates as a function of U(VI) or HNO$_3$ concentration in the organic phase for the samples of series 2, 3, and 4, respectively.

Figure 3 shows the values of the gyration radius and of the two axes of the ellipsoidal aggregates as a function of U(VI) or HNO$_3$ concentration in the organic phase for the samples of series 2, 3, and 4, respectively. The data indicate that particle growth upon HNO$_3$ extraction or UO$_2$(NO$_3$)$_2$ addition to the TBP solution takes place almost entirely along the parallel axis. Similarly, when UO$_2$(NO$_3$)$_2$ is extracted by a TBP·HNO$_3$ solution, further modest growth occurs along the same direction. The largest aggregates exist, as expected, in sample 4c (LOC), with the parallel axis reaching a maximum length of about 64 Å, equal to approximately twice that for the TBP species in sample 1. Upon phase splitting, the aggregates that are present in the heavy and light organic phase exhibit a shorter (much shorter for the third phase sample) parallel axis than that of the LOC sample.

Table 3 also reports calculated values of n$_w$. These values were obtained by using mass-balance equations and the following expression for the weight average aggregation number[24]:

$$n_w = \frac{\sum_n n^2[(TBP)_n]}{\sum_n n[(TBP)_n]} \tag{6}$$

where [(TBP)$_n$] is the organic phase concentration of each n-mer of TBP with or without HNO_3 and/or U(VI). In the calculations it has been assumed that free, unbound TBP exists either as a monomer or as a dimer with a dimerization constant of 2.6.[25] It has also been assumed that the U(VI)-TBP entities should be pentameric in TBP, as indicated by the experimental n_w value for sample 2c in Table 3, and finally, that the HNO_3-TBP particles are tetrameric in TBP (pentameric at saturation), as indicated by the experimental results for samples 3d and 3e.

Under these assumptions, most experimental n_w values are successfully replicated by the calculations. It is encouraging that for sample 1, a quite good match is obtained between the experimental n_w value and the one calculated by using the literature dimerization constant of TBP.[25]

The presence of pentameric TBP aggregates may, of course, reflect the coexistence in solution of tetrameric and hexameric TBP species in equilibrium. The existence of particles that are hexameric in TBP seems likely, based on the n_w values for samples 4a and 4c in Table 3, which are higher than 5. Following introduction of nitric acid and uranyl nitrate in the system, these particles may be formed, for example through self-assembly along the parallel axis, of up to a maximum of three $UO_2(NO_3)_2{\cdot}(TBP)_2$ molecules each containing two TBP molecules.

The third phase sample, however, represents a particular case. Since the composition of sample 4d is $UO_2(NO_3)_2{\cdot}(TBP)_2{\cdot}HNO_3$, with two TBP molecules bound to each U atom, the lowest calculated value of n_w, assuming no aggregation of the third phase species, should obviously be 2.0. The reason for the discrepancy between experimental and calculated n_w values lies in the fact that the SANS data for this sample must be considered from a different standpoint. The third phase, in fact, should more appropriately be described as a solution of D-dodecane in $UO_2(NO_3)_2{\cdot}(TBP)_2{\cdot}HNO_3$ as the diluent.

From the analytical data in Table 1 and the density of the third phase, the D-dodecane concentration in the third phase (1.33 M) and the density of $UO_2(NO_3)_2{\cdot}(TBP)_2{\cdot}HNO_3$ (1.35 g/mL) were obtained. The scattering length density of $UO_2(NO_3)_2{\cdot}(TBP)_2{\cdot}HNO_3$ ($9.094 \times 10^9\,cm^2$) was calculated by including the contribution of all atoms that take part in the third phase species. This value was used, together with the scattering length density of D-dodecane, in eq. 7:

$$n_{w,D-dod} = \frac{6.022 \times 10^{26} d^2_{D-dod} I(0)}{[D-dodecane](\rho_p - \rho_s)^2 MW^2_{D-dod}} \tag{7}$$

to calculate $n_{w,D\text{-}dod}$, which represents the average number of D-dodecane molecules contained in small pockets of dodecane in the third phase (in eq. 7, $d_{D\text{-}dod}$ and $MW_{D\text{-}dod}$ are density and molecular weight of D-dodecane, respectively). By following this approach, a $n_{w,D\text{-}dod}$ value of 1.9 ± 0.2 was obtained. Based on this result, the third phase solution can be described as a continuous $UO_2(NO_3)_2{\cdot}(TBP)_2{\cdot}HNO_3$ phase with interdispersed pockets of D-dodecane, each containing an average of two D-dodecane molecules.

This conclusion is fully compatible with the primary information provided by the SANS data, that is, the radius of gyration of the dissolved entities. By taking the C–C and C–H distances in the dodecane molecule equal to 1.54 and 1.11 Å, respectively,[26] it can be shown from simple trigonometric considerations that two contiguous extended dodecane molecules can be represented by a cylinder with a radius of 1.11 Å and a length of 32 Å. The radius of gyration of such a cylinder (for cylindrical particles $R_g = \sqrt{(R^2/2 + L^2/12)}$ where R and L are radius and length, respectively) is equal to 9.3 Å, which compares favorably with the value of 9.6 ± 1.0 (see Table 2) obtained from the Guinier analysis of the data for the third phase sample.

CONCLUSION

Chemical analyses have indicated that, under the experimental conditions of this work, HNO_3 is extracted by 20% TBP in D-dodecane primarily as $TBP{\cdot}HNO_3$. When $UO_2(NO_3)_2$ is extracted by $TBP{\cdot}HNO_3$, for each mole of $UO_2(NO_3)_2$ entering the organic phase, two moles of HNO_3 are displaced from it. This is consistent with the hypothesis that the uranium salt forms with TBP the $UO_2(NO_3)_2{\cdot}(TBP)_2$ adduct. On the other hand, under the conditions used in this work to induce phase splitting, the third phase species has the $UO_2(NO_3)_2{\cdot}(TBP)_2{\cdot}HNO_3$ composition.

Small-angle neutron scattering measurements on D-dodecane solutions containing only TBP, or TBP loaded with increasing amounts of HNO_3 and/or U(VI), provided information on size and shape of the particles in solution.

TBP alone, that is, without contacting water or nitric acid, forms small dimeric aggregates, in agreement with research information. When solid $UO_2(NO_3)_2$ is dissolved in TBP, the extractant can be saturated with U(VI) without phase splitting. In this case, ellipsoidal aggregates form in the organic solution, each containing up to a maximum of six TBP molecules [three $UO_2(NO_3)_2{\cdot}(TBP)_2$ molecules]. Ellipsoidal aggregates, each containing up to an average of five $TBP{\cdot}HNO_3$ units, are also formed when HNO_3 is extracted by the TBP solution. Formation of the same type of aggregates is also observed when both HNO_3 and $UO_2(NO_3)_2$ are simultaneously present in the TBP phase. In all these aggregates, upon extraction of either HNO_3 or $UO_2(NO_3)_2$ or both, growth takes place mostly along the long axis of the ellipsoid. The largest aggregates (*a* axis = 15 Å, *b* axis = 64 Å) are those observed in a solution having the highest, or limiting, organic metal concentration (LOC) that is possible to achieve without phase splitting, under a given set of conditions.

Upon third phase formation, the SANS data reveal the presence of smaller aggregates in both the heavy and light organic phase. In the light phase, these aggregates are similar to those observed in solution before phase separation. This result was expected since, as indicated by its composition and by the SANS results, the light phase is nothing else than a different LOC solution, where the TBP concentration is lower (0.51 M) than that in the initial organic phase (0.73 M). The heavy organic phase can be described as a continuous $UO_2(NO_3)_2{\cdot}(TBP)_2{\cdot}HNO_3$ phase with interdispersed pockets each containing an average of two molecules of D-dodecane.

Based on these results, it seems reasonable to conclude that, although formation of relatively large nanosize aggregates before phase splitting is verified, third phase formation in the U(VI)-HNO_3/TBP-*n*-dodecane system is only indirectly caused by solute aggregation. More likely, the TBP system behaves similarly to the N,N'-dimethyl-N,N'-dibutyl-2-tetradecyl-malonamide (DMDBTDMA) system recently investigated by French workers.[3,11,27]

TBP is known to be active at water/oil interfaces, especially when bound to water, inorganic acids or metal salts.[28] It is not surprising, therefore, that upon extraction of HNO_3 and/or $UO_2(NO_3)_2$, the TBP species self-assemble in elliptical aggregates having a polar core, similar to reverse micelles, where the hydrophilic $P=O$ groups bound to HNO_3 and U(VI) are located. In analogy to the DMDBTDMA case,[3,11,27] the aggregates contain only a small number (from 4 to 6) of extractant molecules. The polar core of these stable aggregates swells with an increase of the concentrations of extracted acid and metal, up to the size observed for the LOC solution.

A dramatic change in solution leading to phase splitting takes place when, by increasing the aqueous acid concentration in equilibrium with the organic phase, one molecule of HNO_3 becomes part of the U(VI)-TBP complex. The introduction of this excess HNO_3 into the polar core of the aggregate probably increases the solubility parameter of the solute species beyond the value compatible with solubility in dodecane. At this point, the closed structure of the swollen aggregated is disrupted, and some of the solute, in which all TBP molecules are now bound to both U(VI) and HNO_3, separates in a different phase (probably highly structured) from which all the dodecane has been expelled, except for few molecules dispersed in the third phase as small pockets.

ACKNOWLEDGMENTS

This work was funded by the U. S. Department of Energy, Office of Basic Energy Science, Division of Chemical Science (for the part performed at the Chemistry Division of ANL) and Division of Material Science (for the part performed at INPS), under contract No. W-31-109-ENG-38.

The authors express their gratitude to Denis Wozniak (IPNS) for the help provided in the SANS measurements. The authors also thank Paul Rickert, Alice Essling, and Susan Lopykinski of ANL for the purification of the TBP sample used in this work and for uranium and water analyses.

REFERENCES

1. Marcus, Y.; Kertes, A.S. *Ion Exchange and Solvent Extraction of Metal Complexes*; Wiley Interscience: New York, 1969; 715.
2. Asseo-Asare, K. Third phase formation in solvent extraction: a microemulsion model. In *Metal Separation Technologies Beyond 2000: Integrating Novel Chemistry with Processing*; Liddel, K.C., Chaiko, D.J., Eds.; The Minerals, Metals & Materials Society, 1999.
3. Lefrançois, L.; Belnet, F.; Noel, D.; Tondre, C. An attempt to theoretically predict third phase formation in the dimethyldibutyltetradecylmalonamine (DMDBTDMA)/dodecane/water/nitric. Sep. Sci. Technol. **1999**, *34* (5), 755–770.
4. Vasudeva Rao, P.R.; Kolarik, Z. A review of third phase formation in extraction of actinides by neutral organophosphorus extractants. Solvent Extr. Ion Exch. **1996**, *14* (6), 955–993.
5. Kertes, A.S. The chemistry of the formation and elimination of a third phase in organophosphorus and amine extraction systems. *Solvent Extraction Chemistry of Metals*; McMillan: London, 1965; 377–399.
6. Chiarizia, R.; Urban, V.; Thiyagarajan, P.; Herlinger, A.W. Aggregation of P,P$'$-di(2-ethylhexyl) methanediphosphonic acid and its Fe(III) complexes. Solvent Extr. Ion Exch. **1998**, *16* (5), 1257–1278.
7. Chiarizia, R.; Urban, V.; Thiyagarajan, P.; Herlinger, A.W. Aggregation of complexes formed in the extraction of selected metal cations by

P,P′-di(2-ethylhexyl) methanediphosphonic acid. Solvent Extr. Ion Exch. **1999**, *17* (1), 113–132.

8. Chiarizia, R.; Urban, V.; Thiyagarajan, P.; Herlinger, A.W. SANS study of aggregation of complexes formed in the extraction of selected metal cations by P,P′-di(2-ethylhexyl) ethane- and butane-diphosphonic acids. Solvent Extr. Ion Exch. **1999**, *17* (5), 1171–1194.
9. Thiyagarajan, P.; Diamond, H.; Horwitz, E.P. Small-angle neutron scattering studies of the aggregation of Pr(NO3)3-CMPO and PrCl3-CMPO complexes in organic solvents. J. Appl. Cryst. **1988**, *21*, 848–852.
10. Diamond, H.; Thiyagarajan, P.; Horwitz, E.P. Small-angle neutron scattering studies of praseodymium-CMPO polymerization. Solvent Extr. Ion Exch. **1990**, *8* (3), 503–513.
11. Erlinger, C.; Gazeau, D.; Zemb, T.; Madic, C.; Lefrançois, L.; Hébrant, M.; Tondre, C. Effect of nitric acid extraction on phase behavior, microstructure and interactions between primary aggregates in the system dimethyldibutyltetradecylmalonamide (DMDBTDMA)/n-dodecane/water: a phase analysis and small-angle x-ray scattering (SAXS) characterisation study. Solvent Extr. Ion Exch. **1998**, *16* (3), 707–738.
12. Healy, T.V.; McKay, H.A.C. The extraction of nitrates by tri-n-butylphosphate (TBP). Part 2. The nature of the TBP phase. Trans. Faraday Soc. **1956**, *52*, 633–642.
13. Solovkin, A.S.; Povitskii, N.S.; Lunichkina, K.P. Formation of a third phase in the system UO2 (NO3)2-HNO3-H2O-tri-n-butylphosphate-kerosene. Russian J. Inorg. Chem. **1960**, *5* (9), 1026–1028, (English Transl.).
14. Boukis, N.; Kanellakopoulos, B. *Extraktive Phasenverteilung des Uranylnitrats mit Tri(n-butyl)phosphat. II. Die Bildung einer dritten Phase im System* $UO_2(NO_3)_2$*-TBP-*HNO_3, Report KfK-3352; Kernforschungszentrum Karlsruhe: Germany, 1983.
15. Thiyagarajan, P.; Epperson, J.E.; Crawford, R.K.; Carpenter, J.M.; Klippert, T.E.; Wozniak, D.G. The time-of-flight small-angle neutron diffractometer (SAD) at IPNS, Argonne national laboratory. J. Appl. Cryst. **1997**, *30*, 280–293.
16. Crawford, R.K.; Thiyagarajan, P.; Epperson, J.E.; Trouw, F.R.; Kleb, R.; Wozniak, D.G.; Leach, D.J. In *The New Small Angle Diffractometer SAND at IPNS*, Proc. 13th International Collaboration on Advanced Neutron Sources, Villingen, Switzerland, Oct 11–14, 1995; PSDI-Proc 95-02, 1997; 99.

17. Guinier, A.; Fournet, G. *Small Angle Scattering of X-Rays*; John Wiley and Sons: New York, NY, 1955.
18. Guinier, A. La Diffraction des Rayons X aux Très Petits Angles: Application à l'Etude de Phénomènes Ultramicroscopiques. Ann. Phys. **1939**, *12*, 161–237.
19. McKay, H.A.C. *Tri-n-butyl Phosphate as an Extracting Agent for the Nitrates of the Actinide Elements*; Proc. Int. Conf. Peac. Uses At. En., Geneva, Aug 8–20, 1955; 1956; Vol. 7, 314–317.
20. Schaekers, J.M. Extraction of inorganic acids. In *Science and Technology of Tributyl Phosphate*; Schulz, W.W., Navratil, J.D., Kertes, A.S., Eds.; CRC Press: Boca Raton, Fl, 1991; Vol. 4, 71–204.
21. Jensen, M.P.; Chiarizia, R.; Ferraro, J.R.; Borkowski, M.; Nash, K.L.; Thiyagarajan, P.; Littrell, K.C. In *New Insights in Third Phase Formation in the U(VI) HNO3, TBP-Alkane System*, Proc. Int. Solv. Extr. Conf. ISEC 2002, Cape Town, South Africa, Mar 18–21, 2002; Sole, K.C., Cole, P.M., Preston, J.S., Robinson, D.J., Eds.; S. African Institute of Mining and Metallurgy: Johannesburg, 2002; 1137–1142.
22. Borkowski, M.; Ferraro, J.R.; Chiarizia, R.; McAlister, D.R. FT-IR study of third phase formation in the U(VI) or Th(IV)/HNO_3, TBP/alkane systems. Solvent Extr. Ion Exch., **2002**, *20*, 313–330.
23. Pedersen, J.S. Analysis of small-angle scattering data from colloids and polymer solutions: modeling and least-squares fitting. Adv. Colloid Interface Sci. **1997**, *70*, 171–210.
24. Young, R.J.; Lovell, P.A. *Introduction to Polymers*, 2nd Ed.; Chapman-Hall: London, 1991; 11–14.
25. Vandegrift, G.F. Diluents for TBP extraction systems. In *Science and Technology of Tributyl Phosphate*; Schulz, W.W., Navratil, J.D., Kertes, A.S., Eds.; CRC Press: Boca Raton, Fl, 1984; Vol. 1, 69–136.
26. *Handbook of Chemistry and Physics*, 64th Ed.; CRC Press: Boca Raton, Fl, 1983–1984.
27. Lefrançois, L.; Delpuech, J.J.; Hébrant, M.; Chrisment, J.; Tondre, C. Aggregation and protonation phenomena in third phase formation: an nmr study of the quaternary malonamide/dodecane/nitric acid/water system. J. Phys. Chem. **2001**, *105*, 2551–2564.
28. Cox, M.; Flett, D.S. In *The Significance of Surface Activity in Solvent Extraction Reagents*, Proc. Int. Solv. Extr. Conf. ISEC 77, Cim Special Volume 21, The Canadian Institute of Mining and Metallurgy, Montreal, 1977; 63–72.